HHS Public Access

Author manuscript

Biomaterials. Author manuscript; available in PMC 2016 March 01.

Published in final edited form as:

Biomaterials. 2015 March ; 44: 103–110. doi:10.1016/j.biomaterials.2014.12.019.

Prolonged Prevention of Retinal Degeneration with Retinylamine Loaded Nanoparticles

Anthony Puntel[1], **Akiko Maeda**[2,3], **Marcin Golczak**[2], **Song-Qi Gao**[2], **Guanping Yu**[1], **Krzysztof Palczewski**[2], and **Zheng-Rong Lu**[1,*]

[1]Department of Biomedical Engineering, School of Engineering, Case Western Reserve University, Cleveland, Ohio 44140, USA

[2]Department of Pharmacology, Cleveland Center for Membrane and Structural Biology, School of Medicine, Case Western Reserve University, Cleveland, Ohio 44140,USA.

[3]Department of Ophthalmology, School of Medicine, Case Western Reserve University, Cleveland, Ohio 44140, USA.

Abstract

Retinal degeneration impairs the vision of millions in all age groups worldwide. Increasing evidence suggests that the etiology of many retinal degenerative diseases is associated with impairment in biochemical reactions involved in the visual cycle, a metabolic pathway responsible for regeneration of the visual chromophore (11-*cis*-retinal). Inefficient clearance of toxic retinoid metabolites, especially all-*trans*-retinal, is considered responsible for photoreceptor cytotoxicity. Primary amines, including retinylamine, are effective in lowing the concentration of all-*trans*-retinal within the retina and thus prevent retina degeneration in mouse models of human retinopathies. Here we achieved prolonged prevention of retinal degeneration by controlled delivery of retinylamine to the eye from polylactic acid nanoparticles in *Abca4*$^{-/-}$*Rdh8*$^{-/-}$ (DKO) mice, an animal model of Stargardt disease/age-related macular degeneration. Subcutaneous administration of the nanoparticles containing retinylamine provided a constant supply of the drug to the eye for about a week and resulted in effective prolonged prevention of light-induced retinal degeneration in DKO mice. Retinylamine nanoparticles hold promise for prolonged prophylactic treatment of human retinal degenerative diseases, including Stargardt disease and age-related macular degeneration.

Introduction

Progressive retinal degeneration is a leading cause of irreversible vision loss worldwide. It potentially affects a broad age spectrum from Stargardt disease in juveniles to age-related

*Corresponding author, Dr. Zheng-Rong Lu, Department of Biomedical Engineering, Wickenden Building, Room 427, Case Western Reserve University, 10900 Euclid Avenue, Cleveland, OH 44106-7207, zxl125@case.edu.

macular degeneration (AMD) in individuals over 50 years old. Currently, there is no FDA approved treatments of the retinal degenerative diseases. Although diverse in clinical manifestations, many retinal degenerative pathologies are linked to impairments in all-*trans*-retinal (atRAL) clearance from the photoreceptor cells. This process depends on a metabolic pathway called retinoid (visual) cycle, a process involving continuous re-isomerization of atRAL back to its *cis* configuration [1-3]. Continuous recycling of the retinoids is essential for the regeneration of light-sensitive pigments required for vision as well as the health of photoreceptor cells [4]. Inefficient clearance of atRAL by the retinoid cycle results in transient accumulation of this toxic aldehyde and formation of related dimeric products including A2E-like derivatives, resulting in irreversible loss of photoreceptor cells [5-11]. Recent reports have shown that the sequestration of atRAL with primary amines or inhibition of retinoid isomerase (RPE65) can lower retina atRAL concentrations to a safe level and prevent retinal degeneration in *Abca4*$^{-/-}$/*Rdh8*$^{-/-}$ double knockout (DKO) mice, a model for human Stargardt disease and age-related macular degeneration (AMD) [12, 13]. Retinylamine is an amine derivative of retinoids and acts as both an aldehyde scavenger and an inhibitor of RPE65 [14, 15]. It shows the promise to effectively prevent light-induced retinal degeneration in DKO mice. Controlled and sustained delivery of retinylamine to the eye can improve its therapeutic efficacy and provide safe and prolonged protection against retinal degeneration.

Drug delivery to the back of the eye has been a major challenge due to the unique anatomy and physiology of the eye [16-18]. The blood-ocular barrier is a major hurdle for effective intraocular delivery of therapeutics. Ocular implants and scleral plug drug delivery devices are used to overcome the barrier to achieve effective intraocular drug delivery. Unfortunately, these delivery systems are invasive to the eye and have poor patient compliance. Retinylamine is a retinoid derivative and can utilize vitamin A transport machinery including retinoid-binding proteins, receptors, and enzymes to overcome the blood-ocular barrier and to reach the retina after its release from the nanoparticles [19]. Thus, sustained release of retinylamine from a drug delivery system *in vivo* could effectively deliver the drug to the eye and maintain a relatively constant drug concentration in the retina to provide prolonged protect against retinal degeneration [20].

We aimed to develop a safe drug delivery system for controlled release of retinylamine to effectively protect the retina from irreversible degeneration. Polylactic acid (PLA) is a biocompatible and biodegradable polymer that was used in numerous clinical drug delivery systems [21-27]. Incorporation of retinylamine into PLA nanoparticles could provide controlled drug delivery and prolonged prolonged protection against retinal degeneration, Fig. 1. Here, We prepared PLA nanoparticles containing retinylamine and investigated drug delivery efficiency to the eye and hepatic pharmacokinetics in albino C57BL/6J-Tyr wild-type (WT) mice after subcutaneous administration. The therapeutic efficacy of the drug loading nanoparticles was examined in the *Abca4*$^{-/-}$*Rdh8*$^{-/-}$ mouse model *in vivo*.

Results and Discussion

Retinylamine loaded PLA nanoparticles were formulated using single emulsion technique. The drug containing nanoparticles had an average diameter of 730±310 nm with a loading

capacity of 6.9±0.3% (w/w), Fig. 2. The nanoparticles displayed an initial burst of release within the first 24 h and then exhibited zero-order drug release kinetics in PBS (pH 7.4) at 37 °C up to 4 weeks.

The effect of nanoparticle encapsulated retinylamine on modulation of the visual cycle chemistry was examined in concert with the pharmacokinetics of this drug in the eye after subcutaneous administration in 8-week-old albino WT mice. The kinetics of 11-*cis*-retinal (11c-RAL) recovery after light exposure was first investigated in WT mice. To establish a baseline for recovery of 11c-RAL after intensive light exposure, the mice were dark adapted for 24 h prior to 10 min light exposure at 6500 lux. This bright light caused ~90% bleach of the visual chromophore that reduced the at-RAL to all-*trans*-retinol, which was then converted into retinyl esters (Fig. 3a). Efficient regeneration of 11c-RAL was observed within the first few hours after light exposure, and full recovery was achieved after 16 h. These results suggest that any modulation of the visual cycle chemistry by the nanoparticles should be apparent after this time period.

The efficacy of the retinylamine-loaded nanoparticles was investigated in the WT mice according to the experimental procedures schematically depicted in Fig. 3b. Retinoid concentrations were measured 24 h after the light-exposure in different treatment groups. At a retinylamine equivalent dose of 10 mg/kg, subcutaneous administration of retinylamine-loaded nanoparticles resulted in a prolonged constant concentration of retinylamide, a metabolic derivative indicative of the presence of retinylamine in the eye, Fig. 3c,d. It should be noted here that upon treatment with retinylamine, the enzyme lecithin:retinol acyltransferase (LRAT) amidated the drug by transferring a palmitoyl chain from phosphatidylcholine to form the corresponding retinyl amide, a storage form of the drug [28]. The results here suggest that the zero-order sustained release of retinylamine from the nanoparticles maintained a relatively constant drug supply to the eye for up to 7 days (168 h), while retinylamide was not detected 3 days after administration of the free drug. The presence of retinylamine slowed down the retinoid cycle in the retina. Consequently, the concentration of 11c-RAL was maintained at a relatively low level and retinyl esters were at a relatively high level for 7 days with nanoparticles, but only 2 days for the free drug in the WT mice. The results indicate that sustained delivery of retinylamine to the eye by the nanoparticles resulted in more prolonged modulation of retinoid chemistry than the free drug at the same dose.

The hepatic pharmacokinetics of the retinylamine released from nanoparticles was examined in comparison with free retinylamine. The liver is the main storage organ for vitamin A and it is assumed that this also holds true for retinylamine due to their structural similarity. LRAT is also predominantly expressed in the liver. The controlled release of retinylamine from the nanoparticles substantially reduced the hepatic accumulation of the retinylamide as compared to that from free retinylamine, Fig. 4. A low accumulation of retinylamide in the liver could minimize potential dose-related side effects of the drug. We noted that the drug concentration in both the eye and liver was significantly reduced at 168 h after administration, which differed from its *in vitro* long-term release kinetics from the nanoparticles (Fig. 2 and Fig.3c). This discrepancy might be due to the difference between the *in vitro* and *in vivo* environments around the nanoparticles. For example, the presence of

esterases in the subcutaneous environment could catalyze the degradation of the nanoparticles and/or the nanoparticles could be phagocytosed by macrophages [29]. Enzyme-catalyzed degradation and phagocytosis of the nanoparticles could compromise the long-term efficacy of the nanoparticles. Nevertheless, the PLA nanoparticles provided a constant supply of retinylamine to the eye and effectively modulated retinoid chemistry for up to a week after subcutaneous administration of a low drug dosage.

The efficacy of these nanoparticles for preventing light-induced retina degeneration was investigated in 4-week-old DKO mice. Both ATP-binding cassette transporter 4 (Abca4) and all-*trans*-retinol dehydrogenase 8 (Rdh8) are located in photoreceptor cells and play a critical role in the visual cycle by clearing atRAL [30, 31]. *Abca4*$^{-/-}$/*Rdh8*$^{-/-}$ mice with compromised clearance and conversion of atRAL constitute a suitable mouse model for human Stargardt disease and age-related macular degeneration [32]. Dark-adapted DKO mice were subcutaneously injected with either retinylamine or the nanoparticles at a retinylamine equivalent dose of 10 mg/kg, followed by exposure to at 6500 lux white light for 30 min at 1, 6 or 7 days after drug treatment. Untreated mice with and without light exposure were used as controls. Integrity of the retina was determined by using optical coherent tomography (OCT) in live mice from different treatment groups. The retinylamine nanoparticles completely preserved the retina for 6 days with partial preservation at the day 7 after the treatment, whereas free retinylamine only provided 1 day of protection at the equivalent dose, Fig. 5a. The OCT observation was confirmed by immunohistochemistry, which indicated the severity of retinal degeneration in each group, Fig. 4a. The IHC images revealed that the protection of both rod photoreceptor cells, labeled with anti-rhodopsin antibody (red color) and cone photoreceptor cells, labeled with peanut agglutinin (green color), with the nanoparticles for 6 days with partial protection at the day 7. Quantitative analysis of the outer nuclear layer (ONL) thickness in the OCT images across the eye revealed complete ONL preservation for 1 day with the free drug and 6 days with the nanoparticle preparation, Fig. 5b. The protective efficacy of the nanoparticles formulation in DKO mice was consistent with delivery kinetics of retinylamine to the eye shown in the WT animals.

Photoreceptor cell viability and function in different treatment groups were documented by electroretinography (ERG). Fig. 6 shows the scotopic a-wave ERG signals, correlating with rod photoreceptor electrical activity. Healthy photoreceptors will relay electrical signals corresponding to the intensity of the administered light pulse. The nanoparticles provided a complete protective effect of this electrical signal for 6 days, and partial protection at the day 7, but the free drug had a protective effect for only 1 day. These results were consistent with our findings with OCT and immunohistochemistry.

Finally, 11c-RAL as a surrogate measure for rhodopsin concentration and photoreceptor integrity in the eye was quantified to determine if its presence correlated with the protective efficacy of the nanoparticle preparation at the end of the experiment. As shown in Fig. 7, DKOmice exposed to strong light had a substantial decrease of 11c-RAL in the eye as compared to unexposed mice. Free retinylamine maintained a normal level of 11c-RAL for only 1 day. But the nanoparticles formulation preserved the 11c-RAL level for 6 days, which then decreased on the 7th day after the treatment. 11c-RAL levels in the eye

correlated well with both the retina's condition and functions in the different treatment groups.

The retinylamine loaded PLA nanoparticles provided a constant supply of retinylamine to the eye for about a week, resulting in effective modulation of retinoid cycle chemistry, and prolonged prophylactic protection against light-induced retina degeneration in DKO mice after subcutaneous administration. The drug delivery approach is non-invasive to the eye as compared to ocular implants and scleral plugs. Because of its structural similarity to vitamin A, the release retinylamine from the nanoparticles could effectively reach the retina utilizing the vitamin A transport machinery [19] and maintained a relatively constant concentration for about a week. The duration of protective effects by the nanoparticles correlated well to the presence of the drug in the eye. We are aware of the discrepancy between the *in vitro* drug release kinetics and *in vivo* pharmacokinetics and therapeutic efficacy of the nanoparticles. The surface of the nanoparticles can be modified to minimize enzyme catalyzed degradation of the nanoparticles and clearance of the nanoparticles *via* phagocytosis, and to achieve a more prolonged drug release and prophylactic protection of retina. The retinylamine containing nanoparticles are superior to conventional dosage forms, as they can retain *in vivo* drug concentrations at minimally effective therapeutic levels for prolonged periods of time while avoiding potential dose-related toxicity. Since PLA is biocompatible biomaterials, the drug delivery system is promising for further translational development for prolonged prophylactic treatment of human retinal degenerative diseases, including Stargardt disease and age-related macular degeneration.

Conclusion

Subcutaneous administration of retinylamine loaded PLA nanoparticles was effective for sustained delivery of the drug the retina. The nanoparticles were effective to modulate visual cycle chemistry and provided prolonged protection against light-induced retinal degeneration in DKO mice at a relatively low dose. Sustained drug release from the nanoparticles also resulted in low drug concentration in other organs, which could minimize potential toxic side effects of the drug. Thus, these nanoparticles offer a promising option for prolonged prophylactic treatment of human retinal degenerative diseases.

Experimental

Preparation of retinylamine nanoparticles

Poly(*L*-lactic acid) polymers (M_w 91,000-130,000) were obtained from LACTEL Absorbable Polymers (Birmingham, AL). Retinylamine was synthesized and purified according to the method published by Golczak *et al* [15]. Polylactic acid nanoparticles containing retinylamine were fabricated by a single emulsion technique. Briefly, PLA (140-190 kDa) and retinylamine were dissolved in chloroform at 30 mg/mL polymer and 3 mg/mL retinylamine. The polymer/drug solution was then added in a 1:8 v/v ratio to an aqueous solution containing 2.5% w/v PVA (Sigma Aldrich, Inc., St. Louis, MO) and immediately sonicated (S-4000; QSonica, LLC, Newton, CT) to a total of 5000 J to form a stabilized emulsion. The emulsion was magnetically stirred overnight to allow complete evaporation of the solvent and subsequent hardening of the polymer. The hardened

nanoparticles were centrifuged at 20,000 rpm, intermittently washed with distilled water three times, resuspended in purified water, and lyophilized. Nanoparticles were stored at −20 °C prior to experiments. Retinylamine loaded particles were determined by dissolving a known mass (~20 mg) of particles in 1mL at a ratio of 1:9 dimehtylsulfoxide:methanol. The solution was then centrifuged at 15,000 rpm for 10 min. Retinylamine concentration in the supernatant was determined via reversed-phase HPLC (Beckman Ultrasphere-C_{18}; 5 μm; 4.5×250 mm; flow rate of 1.0 mL/min; 65:35 Acetonitrile (0.05% TFA): Water (0.05%TFA); detection at 325 nm). The corresponding area under the curve was correlated to a standard curve to determine the exact concentration within the supernatant. Loading capacity and loading efficiency were calculated as the mass percentage of encapsulated drug in the nanoparticles and mass percentage of encapsulated drug to the total drug used in the preparation.

Scanning electron microscopy

Drops of resuspended particles were placed onto specimen mounts and allowed to settle. The suspensions were then allowed to dry for 24 h under vacuum in the presence of a desiccant. The samples were sputter coated with silver and imaged by scanning electron microscopy at 5 keV (Hitachi S4500). Both particle surface morphology and size were investigated by this means.

In vitro retinylamine release

To measure release kinetics, a known mass (~10 mg) of particles was suspended in 1mL phosphate-buffered saline (PBS, 7.4 pH) solution and gently agitated via inversion at 37°C. At predetermined intervals up to 28 days, 10% of the total volume was removed, centrifuged, and supernatant extracted for analysis. Fresh PBS was added to replace any removed solution. Concentration of retinylamine in the supernatant was determined as described above. Percentage of the released drug was calculated at different time points.

Animal models

Albino C57BL/6J-Tyr wild-type (WT) mice were obtained from Jackson Laboratory (Bar Harbor, ME). *Abca4*$^{-/-}$*Rdh8*$^{-/-}$ mice were obtained as previously described [33]. All mice used in this study were housed in animal facility at the School of Medicine, Case Western Reserve University, where they were maintained either under complete darkness or in a 12 h light/ 12 h dark cycle environment. All animal procedures and experiments were approved by the Case Western Reserve University Animal Care Committees and conformed to both the recommendations of the American Veterinary Medical Association Panel on Euthanasia and the Association of Research for Vision and Ophthalmology.

Determination of 11c-RAL levels *in vivo*

To determine the recovery rate of the visual chromophore after exposure to strong white light, 8-week-old albino C57BL/6J-Tyr WT mice (male and female, n=3 in each group) were dark-adapted for 24 h prior to intense light exposure. Mice were individually exposed to light at 6,500 lux for 10 min. Upon completion of this exposure, the mice were returned to a dark room, euthanized at predetermined time points (0, 2, 10, and 16 h), and their eyes

were collected for retinoid analysis. Retinoid extraction was done manually after homogenizing the eyes in 1 mL of 1:1 ethanol/phosphate buffered saline (PBS) solution containing 40 mM hydroxylamine. Retinoids were extracted in 4 mL hexane, concentrated, and reconstituted to a volume of 400 μL. Then they were separated and detected by normal-phase HPLC with a UV detector at 325 nm (Agilent Zorbax SIL, 5 μm, 4.5x250 mm, 90:10 hexane/ethyl acetate at a flow rate of 1.4 mL/min, Santa Clara, CA). Retinoids extracted from biological samples were quantified based on standard curves representing the relationship between the amounts of injected synthetic standards in pmols to the resulting areas under their chromatographic peaks.

Retinylamine pharmacokinetics and effect on retinoid cycle

The nanoparticles or free retinylamine were subcutaneously injected (10 mg/kg equivalent of retinylamine) into the neck pad of dark-adapted 8-week-old albino C57BL/6J-Tyr WT mice (male and female, n=3 in each group) at predetermined time points prior to light exposure (4, 12, 24, 48, 72, 96, 120, 144 h) as described above. Once light-exposed, mice were returned to the dark room for 24 h to allow regeneration and re-equilibration of retinoids in the eye. Mice then were euthanized and their eyes and livers were extracted for pharmacokinetic analysis. Retinoid concentrations in the eyes were measured as described above. Retinoids in the liver were analyzed in a similar fashion without using hydroxylamine in the extraction. Concentrations of retinylamide in both the eye and liver were determined by normal-phase HPLC at 325 nm (Agilent- Zorbax SIL, 5 μm, 4.5×250 mm, flow rate of 1.4 mL/min, 80:20 hexane/ethyl acetate).

Efficacy of retina protection in DKO mice

Four-week-old DKO mice (male and female, n=5 for each group) were dark adapted for 24 h and then subcutaneously injected with the nanoparticle formulation or retinylamine (10 mg/kg retinylamine) into the neck pad at predetermined time points (1, 6 and 7 days) prior to light illumination. After light exposure at 6,500 lux for 30 min, mice were returned to a dark room for 7 days to allow any retinal pathology to develop. Mice with and without light exposure were used as controls. Mice were sedated by intraperitoneal injection of 20 μL/g of a mixture of ketamine (6 mg/mL) and xylazine (0.44 mg/mL), and their pupils were dilated with 1% tropicamide. Retina integrity was then assessed non-invasively with ultra-high resolution spectral-domain OCT (SD-OCT; Bioptigen, Irvine, CA). Mice were sedated by 20 μL/g body weight intraperitoneal injection of a rodent cocktail mixture of ketamine (6 mg/mL) and xylazine (0.44 mg/mL), their pupils dilated with 1% tropicamide. Mice were then staged on an animal platform to allow for analysis. ONL thickness was measured from OCT images along the horizontal meridian from the nasal to temporal retina. Electroretinograms (ERGs) were recorded by a previously reported method on a universal electrophysiologic system UTAS E-3000 (LKC Technologies, Inc., Gaithersburg, MD). Mice were sedated as described above, and a contact lens electrode placed on each eye. Reference electrode and ground electrode were positioned on the ear and tail, respectively. The mice were then exposed to varying intensities of light pulses (−40, −24, −10, 0, 12.5 dB) and retinal electrical activity measured. At the end of each experiment, the mice were euthanized and their eyes were extracted for the measurement of 11-*cis*-retinal and immunohistochemistry.

Acknowledgments

This work was supported by grant R24EY021126 from the National Eye Institute of the National Institutes of Health (NIH). ZRL is M. Frank Rudy and Margaret Domiter Rudy Professor of Biomedical Engineering and KP is John H. Hord Professor of Pharmacology.

References

1. Kiser PD, Golczak M, Palczewski K. Chemistry of the retinoid (visual) cycle. Chem Rev. 114:194–232. [PubMed: 23905688]
2. Wolf G. A newly discovered visual cycle necessary for vision during continuous illumination. Nutr Rev. 2002; 60:62–5. [PubMed: 11852972]
3. Rando RR. The biochemistry of the visual cycle. Chem Rev. 2001; 101:1881–96. [PubMed: 11710234]
4. Palczewski K. Chemistry and biology of vision. J Biol Chem. 287:1612–9. [PubMed: 22074921]
5. Maeda A, Maeda T, Golczak M, Palczewski K. Retinopathy in mice induced by disrupted all-trans-retinal clearance. J Biol Chem. 2008; 283:26684–93. [PubMed: 18658157]
6. Maeda T, Golczak M, Maeda A. Retinal photodamage mediated by all-trans-retinal. Photochem Photobiol. 88:1309–19. [PubMed: 22428905]
7. Chen Y, Okano K, Maeda T, Chauhan V, Golczak M, Maeda A, et al. Mechanism of all-trans-retinal toxicity with implications for stargardt disease and age-related macular degeneration. J Biol Chem. 287:5059–69. [PubMed: 22184108]
8. Sparrow JR, Fishkin N, Zhou J, Cai B, Jang YP, Krane S, et al. A2E, a byproduct of the visual cycle. Vision Res. 2003; 43:2983–90. [PubMed: 14611934]
9. Sparrow JR, Wu Y, Kim CY, Zhou J. Phospholipid meets all-trans-retinal: the making of RPE bisretinoids. J Lipid Res. 51:247–61. [PubMed: 19666736]
10. Mata NL, Weng J, Travis GH. Biosynthesis of a major lipofuscin fluorophore in mice and humans with ABCR-mediated retinal and macular degeneration. Proc Natl Acad Sci U S A. 2000; 97:7154–9. [PubMed: 10852960]
11. Murdaugh LS, Wang Z, Del Priore LV, Dillon J, Gaillard ER. Age-related accumulation of 3-nitrotyrosine and nitro-A2E in human Bruch's membrane. Exp Eye Res. 90:564–71. [PubMed: 20153746]
12. Maeda A, Golczak M, Chen Y, Okano K, Kohno H, Shiose S, et al. Primary amines protect against retinal degeneration in mouse models of retinopathies. Nat Chem Biol. 8:170–8. [PubMed: 22198730]
13. Kubota R, Boman NL, David R, Mallikaarjun S, Patil S, Birch D. Safety and effect on rod function of ACU-4429, a novel small-molecule visual cycle modulator. Retina. 32:183–8. [PubMed: 21519291]
14. Golczak M, Maeda A, Bereta G, Maeda T, Kiser PD, Hunzelmann S, et al. Metabolic basis of visual cycle inhibition by retinoid and nonretinoid compounds in the vertebrate retina. J Biol Chem. 2008; 283:9543–54. [PubMed: 18195010]
15. Golczak M, Kuksa V, Maeda T, Moise AR, Palczewski K. Positively charged retinoids are potent and selective inhibitors of the trans-cis isomerization in the retinoid (visual) cycle. Proc Natl Acad Sci U S A. 2005; 102:8162–7. [PubMed: 15917330]
16. Zhang K, Zhang L, Weinreb RN. Ophthalmic drug discovery: novel targets and mechanisms for retinal diseases and glaucoma. Nat Rev Drug Discov. 2012; 11:541–59. [PubMed: 22699774]
17. Gaudana R, Jwala J, Boddu SH, Mitra AK. Recent perspectives in ocular drug delivery. Pharm Res. 2009; 26:1197–216. [PubMed: 18758924]
18. Kompella UB, Amrite AC, Pacha Ravi R, Durazo SA. Nanomedicines for back of the eye drug delivery, gene delivery, and imaging. Prog Retin Eye Res. 2013; 36:172–98. [PubMed: 23603534]
19. Sun H. Membrane receptors and transporters involved in the function and transport of vitamin A and its derivatives. Biochim Biophys Acta. 2012; 1821:99–112. [PubMed: 21704730]

20. Yu G, Wu X, Ayat N, Maeda A, Gao SQ, Golczak M, et al. Multifunctional PEG Retinylamine Conjugate Provides Prolonged Protection against Retinal Degeneration in Mice. Biomacromolecules. 2014; 15:4570–8. [PubMed: 25390360]

21. Lee SS, Hughes P, Ross AD, Robinson MR. Biodegradable implants for sustained drug release in the eye. Pharm Res. 2010; 27:2043–53. [PubMed: 20535532]

22. Deng D, Wang W, Wang B, Zhang P, Zhou G, Zhang WJ, et al. Repair of Achilles tendon defect with autologous ASCs engineered tendon in a rabbit model. Biomaterials. 2014; 35:8801–9. [PubMed: 25069604]

23. Deng Y, Saucier-Sawyer JK, Hoimes CJ, Zhang J, Seo YE, Andrejecsk JW, et al. The effect of hyperbranched polyglycerol coatings on drug delivery using degradable polymer nanoparticles. Biomaterials. 2014; 35:6595–602. [PubMed: 24816286]

24. Alvarez Z, Castano O, Castells AA, Mateos-Timoneda MA, Planell JA, Engel E, et al. Neurogenesis and vascularization of the damaged brain using a lactate-releasing biomimetic scaffold. Biomaterials. 2014; 35:4769–81. [PubMed: 24636215]

25. Ye F, Barrefelt A, Asem H, Abedi-Valugerdi M, El-Serafi I, Saghafian M, et al. Biodegradable polymeric vesicles containing magnetic nanoparticles, quantum dots and anticancer drugs for drug delivery and imaging. Biomaterials. 2014; 35:3885–94. [PubMed: 24495486]

26. Ma X, Cheng Z, Jin Y, Liang X, Yang X, Dai Z, et al. SM5-1-conjugated PLA nanoparticles loaded with 5-fluorouracil for targeted hepatocellular carcinoma imaging and therapy. Biomaterials. 2014; 35:2878–89. [PubMed: 24411331]

27. Zhang X, Dong Y, Zeng X, Liang X, Li X, Tao W, et al. The effect of autophagy inhibitors on drug delivery using biodegradable polymer nanoparticles in cancer treatment. Biomaterials. 2014; 35:1932–43. [PubMed: 24315578]

28. Golczak M, Imanishi Y, Kuksa V, Maeda T, Kubota R, Palczewski K. Lecithin:retinol acyltransferase is responsible for amidation of retinylamine, a potent inhibitor of the retinoid cycle. J Biol Chem. 2005; 280:42263–73. [PubMed: 16216874]

29. Mathaes R, Winter G, Besheer A, Engert J. Influence of particle geometry and PEGylation on phagocytosis of particulate carriers. Int J Pharm. 2014; 465:159–64. [PubMed: 24560647]

30. Molday RS, Beharry S, Ahn J, Zhong M. Binding of N-retinylidene-PE to ABCA4 and a model for its transport across membranes. Adv Exp Med Biol. 2006; 572:465–70. [PubMed: 17249610]

31. Rattner A, Smallwood PM, Nathans J. Identification and characterization of all-trans-retinol dehydrogenase from photoreceptor outer segments, the visual cycle enzyme that reduces all-trans-retinal to all-trans-retinol. J Biol Chem. 2000; 275:11034–43. [PubMed: 10753906]

32. Maeda A, Maeda T, Golczak M, Chou S, Desai A, Hoppel CL, et al. Involvement of all-trans-retinal in acute light-induced retinopathy of mice. J Biol Chem. 2009; 284:15173–83. [PubMed: 19304658]

33. Maeda A, Golczak M, Chen Y, Okano K, Kohno H, Shiose S, et al. Primary amines protect against retinal degeneration in mouse models of retinopathies. Nat Chem Biol. 2012; 8:170–8. [PubMed: 22198730]

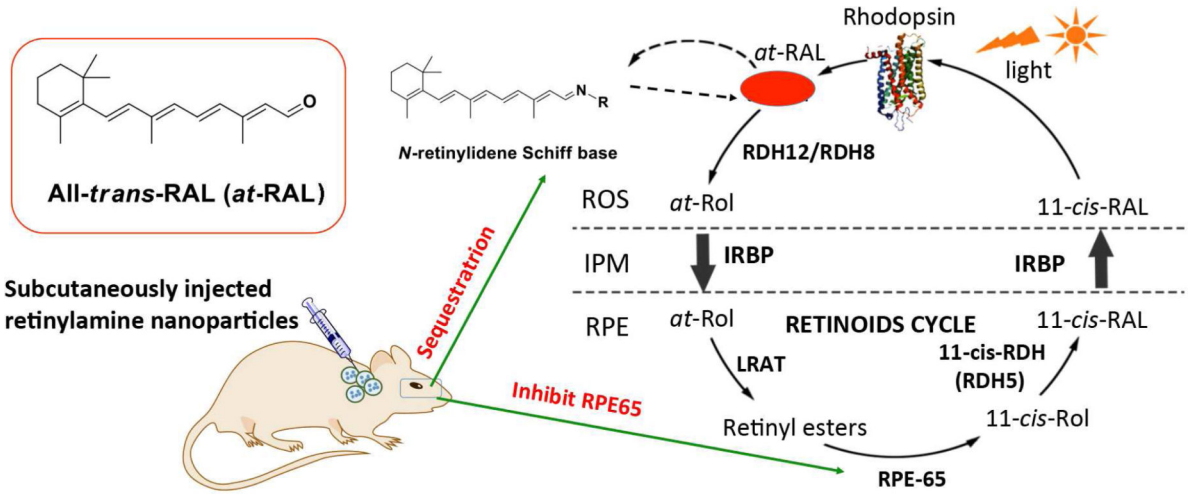

Fig 1.

Retinylamine loaded PLA nanoparticles for prolonged protection against light-induced retinal degeneration in *Abca4*$^{-/-}$*Rdh8*$^{-/-}$ mice. After subcutaneous administration of the biodegradable nanoparticles, retinylamine is gradually released in the body and a sufficient amount of the drug is available in the eye to sequester all-trans-retinal (*at*-RAL) for a prolonged period to effectively protect against light-induced retinal degeneration.

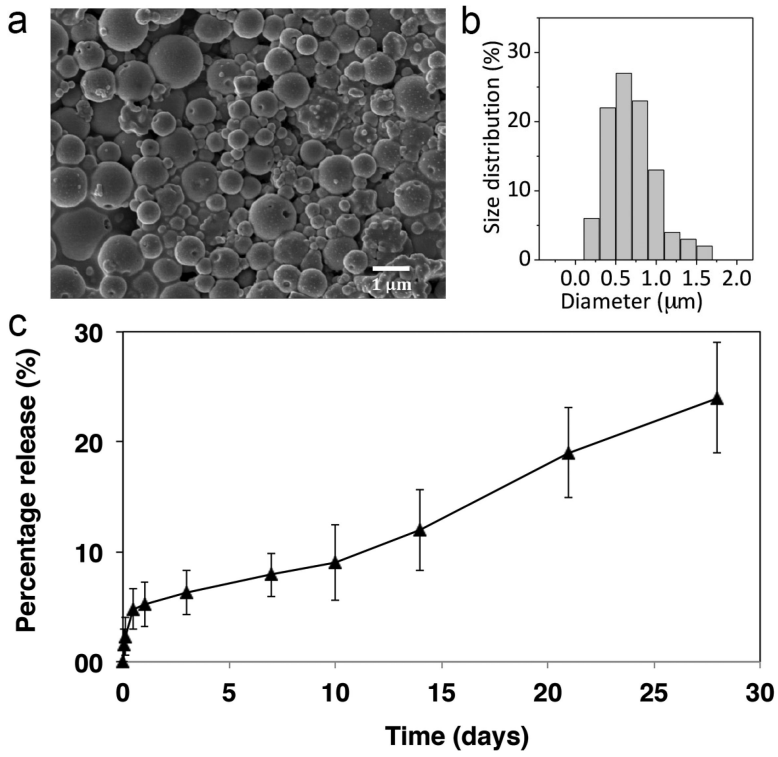

Figure 2.

SEM image (a) and size distribution (b) of the retinylamine loaded PLA nanoparticles. In vitro drug release kinetics of retinylamine from the PLA nanoparticles (c, N=5).

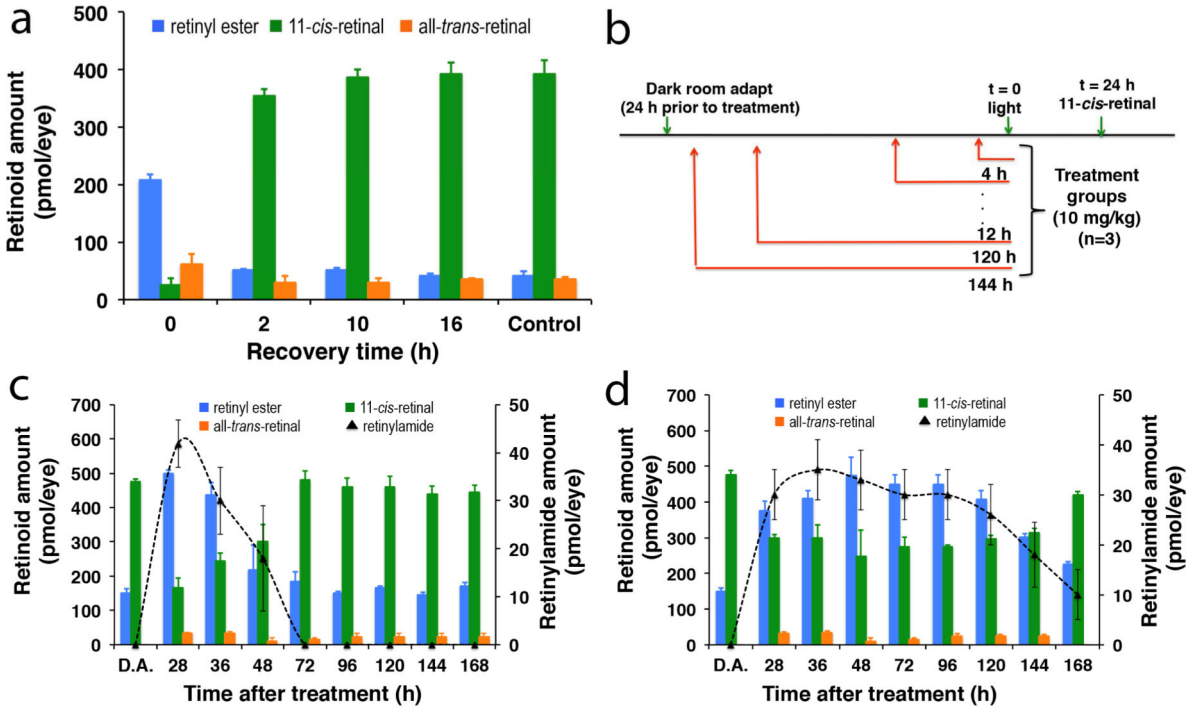

Figure 3.

a) *In vivo* 11-*cis*-retinal recovery rate after strong light exposure in C57BL/6J-Tyr WT mice (N=3). After 24 hours in dark, the mice were exposed to intense light to isomerize 11-*cis*-retinal and develop a baseline recovery rate for the retinoid cycle. Mice were sacrificed at several time intervals (0, 2, 10, 16 hours) to quantify the amount of retinoids in the eye via HPLC analysis. Control mice were not exposed to light and therefore represent the maximum levels of 11-*cis*-retinal; b) experimental plan of the pharmacokinetics of the retinylamine-loaded nanoparticles and their effect on retinoinds after strong light exposure; the amount of retinoids in the eye at different time points in response to strong light exposure after subcutaneous injection of retinylamine (c) and retinylamine-loaded nanoparticles (d) into the dorsal neck pad at a retinylamine equivalent dose of 10 mg/kg (N=3).

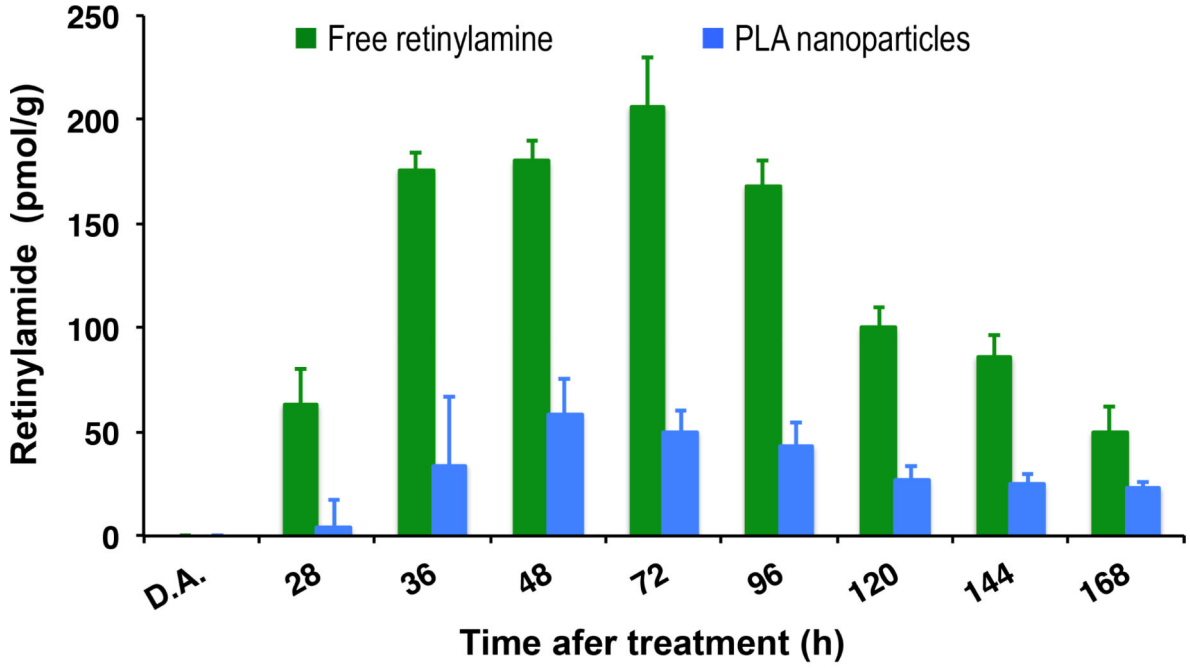

Figure 4.
Hepatic pharmacokinetics of free retinylamine and retinylamine-loaded particles (N=3).

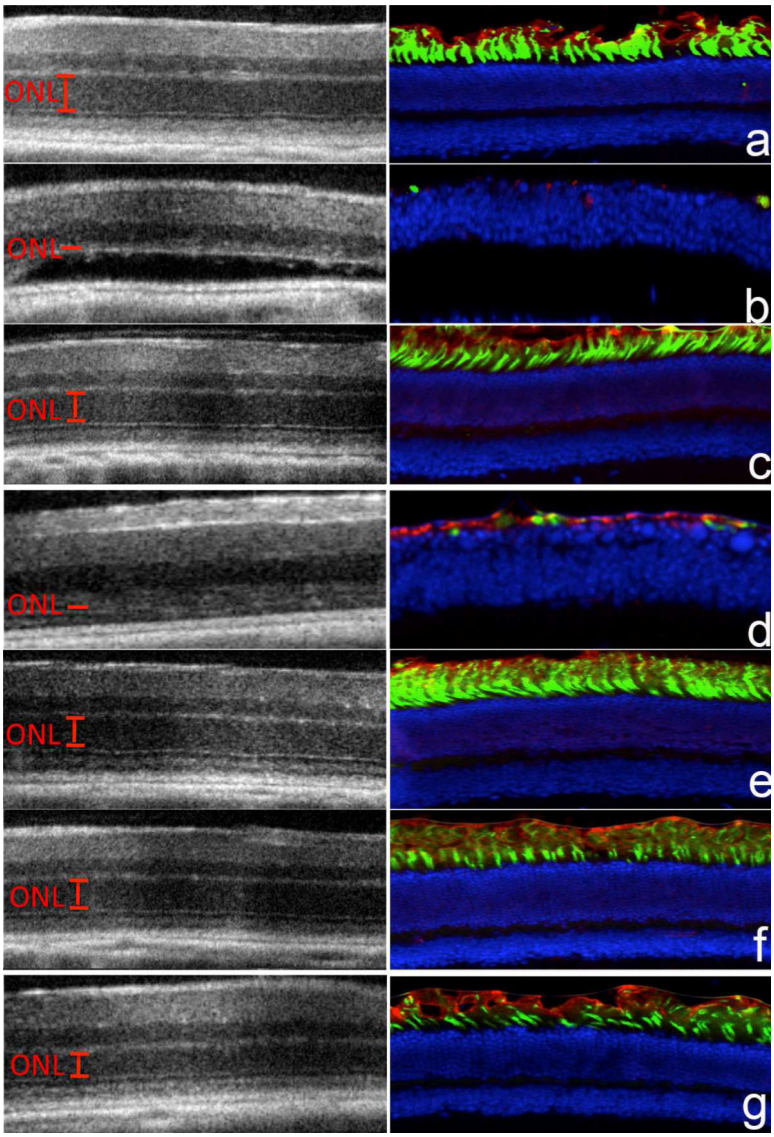

Figure 5.

OCT images (left column, a-g) and immunohistochemical analysis (right column, a-g) of the eyes and the average outer nuclear layer thickness (h) of the retinas measured from the OCT images of DKO mice in the positive control group (a and ◇, no light exposure), the negative control group (b and ◇, light exposure), the group treated with free retinylamine 1 day prior to light exposure (c and Δ), the group treated with the free drug 6 days prior to light exposure (d and green filled triangle), the group treated with the retinylamine PLA nanoparticles 1 day prior to light exposure (e and ○), the group treated with the PLA nanoparticles 6 days prior to light exposure (f and ●), the group treated with the PLA nanoparticle 7 days prior to light exposure (g and ◇). Retinylamine and retinylamine-loaded nanoparticles were subcutaneous injected into the dorsal neck pad at a retinylamine equivalent dose of 10 mg/kg (N = 5).

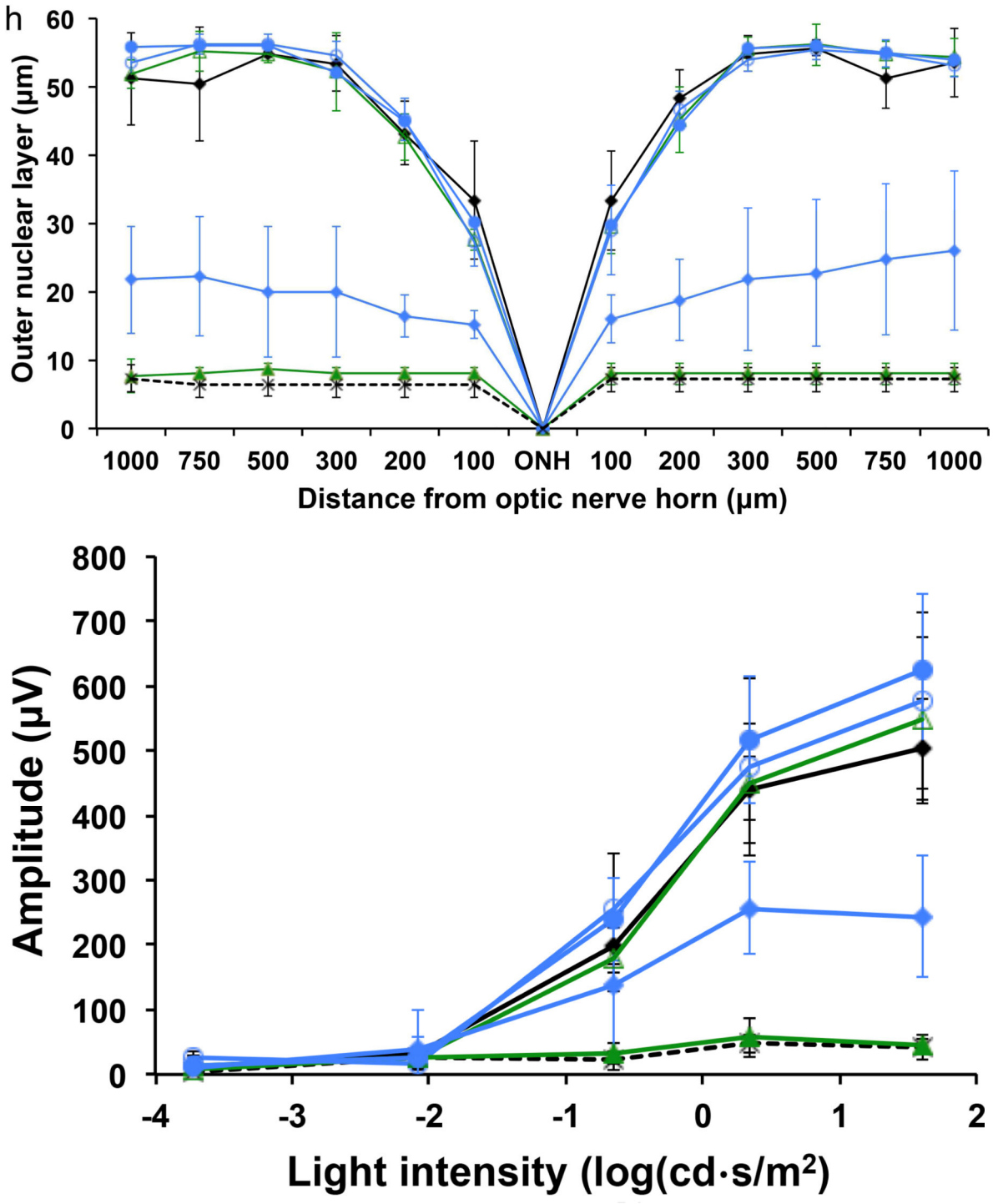

Figure 6.

Scotopic a-wave ERG signals of the eyes of DKO mice in the positive control group (◇, no light exposure), the negative control group, (light exposure), the group treated with free retinylamine 1 day prior to light exposure (Δ), the group treated with the free drug 6 days prior to light exposure (green filled triangle), the group treated with the PLA nanoparticles 1 day prior to light exposure (○), the group treated with the PLA nanoparticles 6 days prior to

light exposure (●), the group treated with the PLA nanoparticle 7 days prior to light exposure (◇) (N=5).

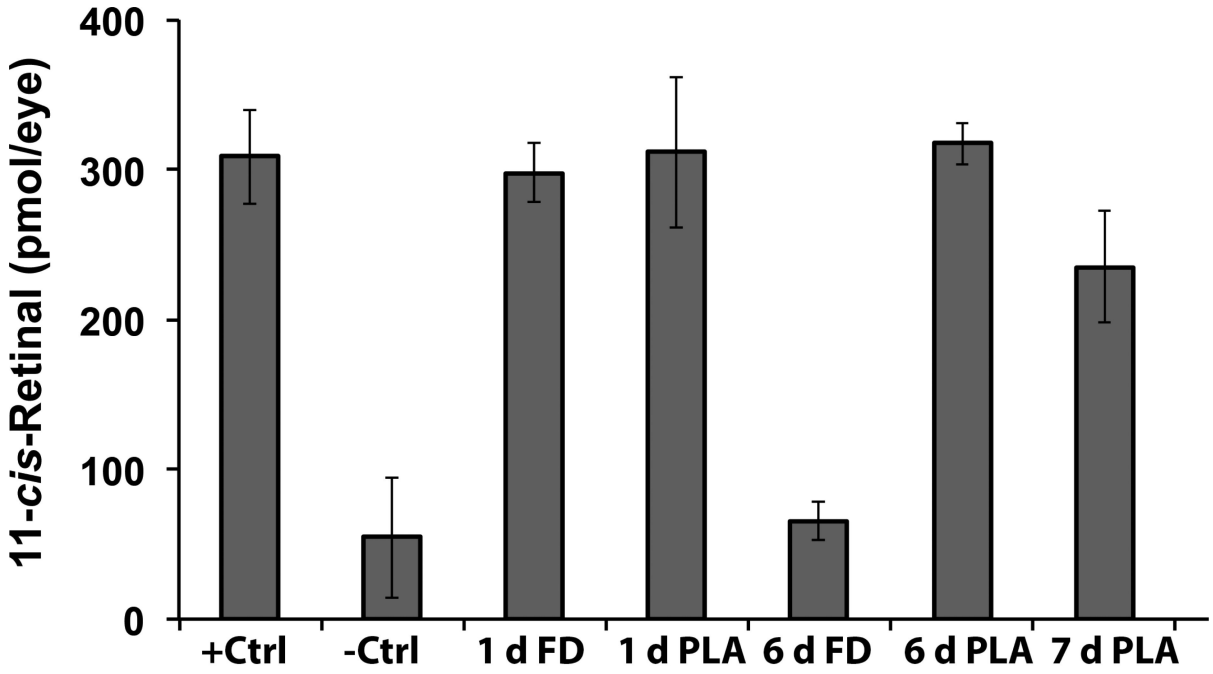

Figure 7.

The concentration of 11-*cis*-retinal in the eyes of DKO mice. Mice in the positive control group with no light exposure (+Ctrl), the negative control group with light exposure (-Ctrl), the group treated with free retinylamine (FD or free drug) 1 day prior to light exposure (1 d FD), the group treated with the PLA nanoparticles 1 day prior to light exposure (1 d PLA), the group treated with the free drug 6 days prior to light exposure (6 d FD), the group treated with the PLA nanoparticles 6 days prior to light exposure (6 d PLA), the group treated with the PLA nanoparticle 7 days prior to light exposure (7 d PLA). (N=5).